

CHAPTER 2

3D Structure of Myosin Crossbridges in Insect Flight Muscle:

Toward Visualization of the Conformations during Myosin Motor Action

Mary C. Reedy

Abstract

Insect flight muscle (IFM) provides a model system that allows direct viewing of individual myosin head structures in situ that give rise to the average structures reported by X-ray patterns and by the mechanical behavior of the fibers. Coordinating X-ray diffraction, physiological monitoring and fast freezing with EM tomography, correspondence class averaging and atomic model building in IFM is providing 3D imaging of different myosin conformations in situ in relaxed, active and rigor states. Rigor has yielded the most detailed 3D structure, showing actin, myosin S2 and a distribution of variously flexed myosin lever arm in class averages. EM tomograms of fast frozen/freeze substituted isometric and stretch-activated contractions show that crossbridges in active contraction bind to actin target zones by only one head, in contrast to the most prominent class of rigor crossbridges that attach with both myosin heads to actin. In contrast to a ~5nm lever arm swing inferred during rigor induction, active myosin heads display a wide range of crossbridge angles, consistent with a power stroke greater than 10nm, that proceeds from a prestroke “up” configuration “down” to a rigor angle. However, measurements of isometrically active IFM crossbridges to determine their position, angle and frequency of attachment to actin indicate that the majority of crossbridges in isometric contraction are angled close to perpendicular to the filament axis (60% within 11°), results that are consistent with X-ray studies of vertebrate isometric contraction. X-ray modeling of ATP relaxed *Lethocerus* IFM shows that a myosin head conformation similar to “prestroke” crystal structures, is arrayed in the 14.5nm periodic “shelves” along thick filaments such that only one head of each molecule is well-positioned, as if poised to bind to actin upon activation, while the other head curves around the thick filament shaft.

Introduction

The indirect flight muscles (IFM) of certain insects, in particular that of the giant waterbug, *Lethocerus*, and the tiny fruit fly *Drosophila*, have presented a treasure trove of information about the structure and function of the actin/myosin molecular motor in situ. IFM presents a unique opportunity to view myosin heads in 3D as they generate tension in the intact muscle lattice. Actin and myosin show an almost crystalline order and lattice arrangement in IFM that makes it an excellent subject for 3D reconstruction. Furthermore, *Lethocerus* IFM is composed of very long (1 cm) parallel fibers. This, combined with the high degree of ordering, make it

ideal for X-ray diffraction studies that can be coordinated with 3D reconstructions from thin section electron microscopy. *Drosophila* IFM is similarly well-ordered but is less than 1 mm in length. *Drosophila*'s small size has allowed X-ray diffraction of IFM in living flies¹ (see also chapter by Irving in this volume) and detailed study of IFM development during pupation.^{2,3} The accessibility of *Drosophila* IFM for genetic manipulation of contractile proteins is unparalleled^{4,5-9} and the structural effects of a number of mutants in contractile proteins have been described.¹⁰⁻¹⁶ However, the most detailed structural studies of crossbridges have focused on *Lethocerus* IFM and these will be discussed in this chapter.

In 1965, Reedy, Holmes and Tregear¹⁷ showed with coordinated X-ray diffraction and electron microscopy (EM) that in glycerinated *Lethocerus* IFM relaxed in MgATP and low calcium (pCa 6.5), myosin heads appeared to project at a $\sim 90^\circ$ angle from "shelves" every 14.5 nm along the thick filaments. When rigor was produced by washing ATP out of the muscle, the myosin heads formed $\sim 45^\circ$ angled crossbridges in a regular pattern of "chevrons" every 38.7 nm along the actin thin filaments (Fig. 1). Measurements of IFM fibers on a force transducer showed that induction of rigor produced substantial stiffness and tension, suggesting that rigor showed the myosin heads at the end of a power stroke. X-ray diffraction patterns indicated that crossbridge mass was concentrated at the 14.5 nm periodicity in ATP-relaxed, while in rigor, the large intensity increase on 38.7 nm layer line and intensity decrease on the 14.5 nm layer line were best modelled and matched by the angled crossbridges attached every 38.7 nm to the thin filament. These results supported the models of sliding filaments and independent force generators¹⁸⁻²¹ and the swinging crossbridge hypothesis.²² X-ray patterns recording the transition between relaxed and rigor IFM from recent studies²³ (Fig. 2) reflect a striking rearrangement of myosin heads and S2 by conversion of 4-fold myosin head origins to 2-fold origins, discussed below.

Advances in instrumentation and techniques have enabled experiments that have filled out and altered this early picture of the tilting power stroke of the myosin crossbridge. For almost three decades, various strategies, including chemical fixation and nucleotide analogs, were used to accumulate static arrays of IFM crossbridges in equilibrium states thought to mimic intermediate stages of a power stroke, seeking to visualize the hypothesized tilting of myosin heads from 90° to 45° .²⁴⁻²⁶ Figure 3 compares crossbridge structures in electron micrographs and EM tomograms obtained from tilt series of longitudinal 25 nm "myac" layer sections of rigor and nucleotide-analog (AMPPNP) treated IFM. The rigor lead bridges are the crossbridge pair closer to the M-line in each 38.7 nm axial repeat, while the rear bridges are the pair closer to the Z-line. The lead and rear rigor crossbridges form what is called a "double chevron" motif. In all states observed thus far, in which crossbridges attach to actin, they bind in actin target zones, helically well-oriented segments of the thin filament. In rigor the target zones span about 4 actin protomers along each strand, while in the intermediate nucleotide states, with lower actin affinity, actin target zones appear to span only two or three protomers. In AMPPNP at room temperature, the nucleotide released the rear crossbridges and caused only a small change in axial angle of the lead crossbridges. When fibers were partially relaxed by adding ethylene glycol to AMPPNP, the long sought-after reversal of attached crossbridge angle was achieved: glycol-AMPPNP crossbridges bound to actin target zones with average angles around 90° to the long axis of the filaments.

Electron tomography, a nonaveraging method of 3D reconstruction,^{27,28} succeeded in retaining and displaying the variety of crossbridge forms in these less uniformly ordered intermediate states.^{25,29} At the same time, new methods of averaging were needed to improve signal to noise in the tomograms without "blurring" details or wiping out the variation in structure preserved in the tomograms.³⁰ The newer methods give an improved view of myosin head structure that supported efforts to fit crystallographic structures of myosin heads into the averaged crossbridge envelopes.

X-ray crystallography has provided the highest resolution views of the conformational changes that accompany alterations in the nucleotide state when myosin is not bound to actin.^{31,32-36}

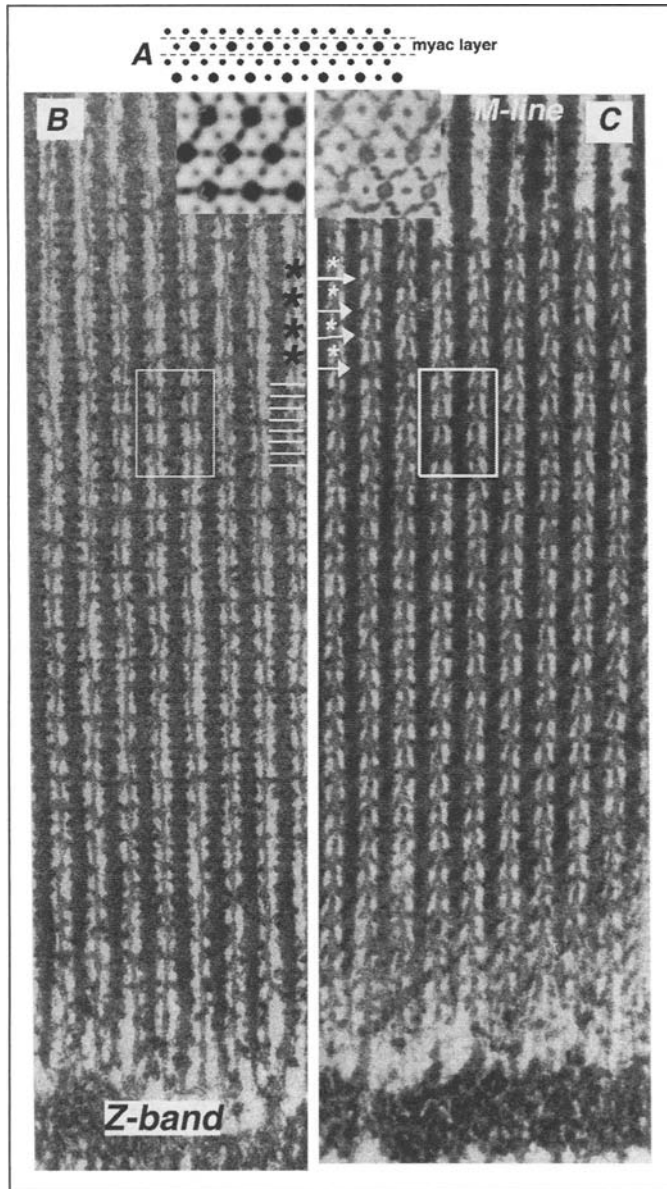


Figure 1. Electron micrographs of 25nm longitudinal sections of *Lethocerus* IFM comparing rigor and ATP-relaxed states at the same magnification. A) Diagram of a cross section view of the hexagonal thick and thin filament lattice of IFM with the actin filaments at the dyad positions between thick filaments. Dashed lines indicate the single filament layer of alternating myosin and actin filaments (myac layer) shown in the longitudinal sections throughout this paper. This arrangement of filaments allows myosin crossbridges to be seen from their origins on the thick filaments to their actin attachments, without inclusion of crossbridges from planes in the hexagonal lattice above or below the myac layer section. B) In ATP-relaxed IFM, the myosin heads form dense shelves every 14.5 nm along the thick filaments that project at a 90° angle toward the thin filaments. At many 38.7 nm intervals, the 90° projections appear to touch the thin filaments at the level of troponin. The figure legend is continued on the next page.

Figure 1, contiued. The black asterisks at the right highlight some of these bridging densities, which are in register across the sarcomere and which coincide with the head regions of troponin. The white lines on the right highlight the levels of eight 14.5 nm shelves, also in register across the sarcomere. The white box includes an 116nm axial repeat, consisting of three 38.7 nm target zones and eight 14.5 nm shelves. The inset shows a ~15 nm cross section view of the relaxed filament lattice that includes only a single "shelf" level on each filament. The thick filaments have a tetragonal outline because the relaxed myosin heads originate from four points around them. C) In rigor, the maximum number of myosin heads attach to actin at each half turn of the actin helix every 38.7 nm to form regular, angled chevrons that point toward the M-line. The alternating white lines and asterisks on the left highlight lead crossbridges (arrows) alternating with the head region of troponin (asterisks), also spaced every 38.7 nm. The white box outlines two thin/thick filament corridors over an 116nm axial repeat containing three 38.7 nm chevrons. The most prominent rigor crossbridges, the lead chevrons, bind in the actin target zone midway between the head regions of troponin, which appear as black dots on the thin filament between the chevrons. The inset shows a ~15 nm cross section view of rigor that includes only one level of bridges. Rigor bridges originate from two-fold positions across the thick filament to form the "flared X".

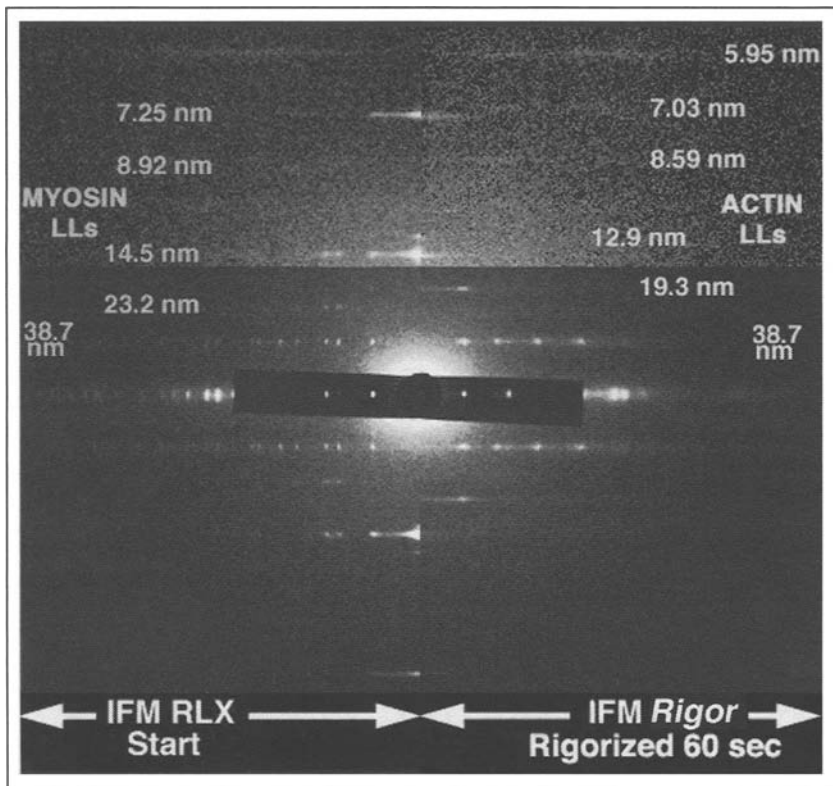


Figure 2. Time resolved synchrotron X-ray diffraction patterns of *Lethocerus* IFM recording the transition in 60 seconds from ATP-relaxed on the left side to rigor on the right. The 14.5 nm and 7.2 nm myosin-based reflections are very strong in relaxed IFM and weak in rigor, and the 38.7 nm and 19.3 reflections become stronger in rigor. As rigor develops, the weakening of the 14.5 nm and 7.2 nm relaxed reflections and the strengthening of the 38.7 nm and 19.3 nm layer lines reflects the striking rearrangement of myosin molecules as they leave the relaxed head array on the thick filament, attach to actin and go through a power stroke to form long-lasting, strong-binding rigor attachments to actin as ATP is exhausted. These synchrotron X-ray patterns were obtained at BIOCAT beamline at APS, Argonne.⁶⁹

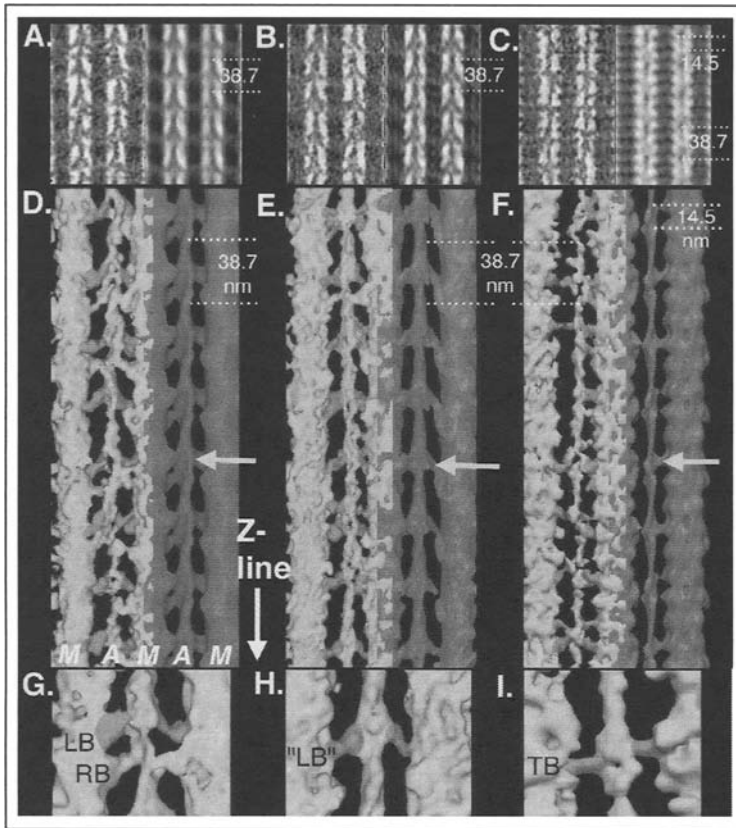


Figure 3. Comparison of *Lethocerus* IFM in chemically fixed, stable equilibrium states of rigor (A,D,G), AMPPNP (B,E,H) and GlycolAMPPNP (C,F,I). Electron micrographs (left side) and 2D filtered images (right side) are shown in (A,B,C). Single thin filament corridors from unaveraged tomograms of the respective states are shown on the left in yellow and their column average on the right in red in (D,E,F). Chartreuse arrows point to crossbridges at the center of the actin target zone (lead bridges (LB) in rigor and AMPPNP; equivalent target zone bridges (TB) in glycolAMPPNP). These bridges are also highlighted orange in the 38.7 nm repeats from the unaveraged tomogram in (G,H,I). RB is rear bridge. M is myosin filament; A is actin filament. Modified from Schmitz et al.^{25,29} A color version of this figure is available online at <http://www.Eurekah.com>.

Crystallographic studies have shown that each myosin head, also known as subfragment 1 (S1), contains the first 843 N-terminal residues of the heavy chain and an essential light chain (ELC) and a regulatory light chain (RLC). Each S1 consists of a motor domain that contains the actin binding and ATPase sites and a light chain domain (LCD), a long alpha-helical segment of the myosin heavy chain encircled by one ELC and one RLC. Several models of the myosin working stroke^{37,38} based on X-ray crystal structures propose that the LCD serves as a lever arm to amplify the small conformational changes in the motor domain driven by ATP-hydrolysis and product release. Figure 4A depicts the superimposition on one motor domain of the S1 crystal structures of the prestroke conformation³⁴ with bound nucleotide and the Rayment et al³² nucleotide-free rigor conformation. The transition between the "up" and "down" positions of the lever arms suggested a 10.5 nm myosin power stroke. Different LCD positions consistent with the tilting lever arm hypothesis have been observed in acto-S1^{39,40} and in actively contracting IFM.⁴¹

Rebuilding the crystal structures of acto-S1 to fit the envelopes of crossbridges in 3D reconstructions provides a link between the single average structure at high resolution obtained by X-ray crystallography of myosin crystals or X-ray diffraction of muscle fibers and lower resolution 3D tomograms that retain individual variations that contribute to the single average. Comparing *in situ* crossbridges to atomic structures of acto-S1 allows workers to infer the position of the motor and lever arm domains of S1 in the crossbridge envelopes. This allows different models of the myosin power stroke derived from X-ray diffraction, crystallography and fiber mechanics to be tested and visualized in muscle fibers.

The Rigor State

The most detailed 3D picture of myosin head conformations comes from rigor, in which the maximum number of myosin heads form stable attachments to actin. Even though myosin heads in rigor are strongly bound to actin at the end of the power stroke, the forms of myosin heads in rigor are expected to reflect a range of structures responsible for active force generation, but in a highly ordered, long-lasting state that facilitates structural analysis. Rigor has served, therefore, as a model for the development of several of the new methodologies. Chemically-fixed rigor IFM that showed excellent order, including preservation of the 5.9 and 5.1 nm actin layer lines in thin sections,⁴² has been extensively utilized for developing averaging methods to apply to EM tomograms. The most recent method is 3D correspondence analysis (or multivariate statistical analysis).^{30,43} Rather than averaging together all variable crossbridge structures throughout the tomogram or along a filament, each 38.7 nm repeat (a 3D crossbridge motif) is demarcated ("masked") in the tomogram. Correspondence analysis then identifies and groups motifs with self-similar 3D crossbridge structures and averages members of each group to form class averages.⁴⁴

Figure 4B shows one class average from a tomogram of IFM in rigor that displays a double chevron. The envelope of the thick and thin filaments and crossbridges are shown in a transparent rendering that allows the rebuilt atomic models of acto-S1 fitted to the envelope to be seen. The lead chevrons, the M-ward crossbridge pair in each 38.7 nm motif, contain both heads of one myosin molecule. The S1 on the M-line side is the M-ward head; the S1 on the Z-line side is the Z-ward head. The Z-ward pair, the rear chevron, usually consists only of a single myosin head in each bridge.

The range of conformations of myosin heads under tension in the intact lattice has been explored by rebuilding the crystal structure of nucleotide-free S1³² to fit rigor crossbridge envelopes in EM tomograms⁴⁴ (Fig. 4B). When S1 heads are bound to actin *in vitro*, the S1 heads are free from the common origin that constrains them in the intact molecule. The C-termini of S1s bound to successive actins are separated both axially and azimuthally (peek ahead to Fig. 5A,B). In contrast to the uniform structure of S1 in crystals or bound to actin *in vitro*, the two S1s in rigor crossbridges that contain both heads of one molecule, show different angles and shapes. The position of the motor domain of the S1 atomic model on actin matches rigor crossbridges, but the orientation of the LCD requires axial, azimuthal and twist adjustments to fit crossbridges.

When the motor domains of all refined S1 models rebuilt to fit chemically fixed rigor crossbridges⁴⁴ are superimposed onto a single actin and motor domain, the range of positions of the C-terminal heavy chain residue of the LCD of the rebuilt S1, K843, can be interpreted as reflecting an accumulation of all lever arm angles occurring during the final power stroke as the fiber enters rigor (Fig. 4C). In the rigor fittings, the positions of K843 on the myosin heavy chains define an arc that covers an axial range of 5-6 nm. The axial angles of the fitted lever arms of single-headed "rear" crossbridges also covered a 5-6 nm range. The range of LCD positions suggests a 5-6 nm lever arm stroke during rigor induction. The range of rigor lever arm angles is similar to the range observed in rebuilt S1 models inferred to be in late-stages of the power stroke in isometrically active IFM.⁴¹

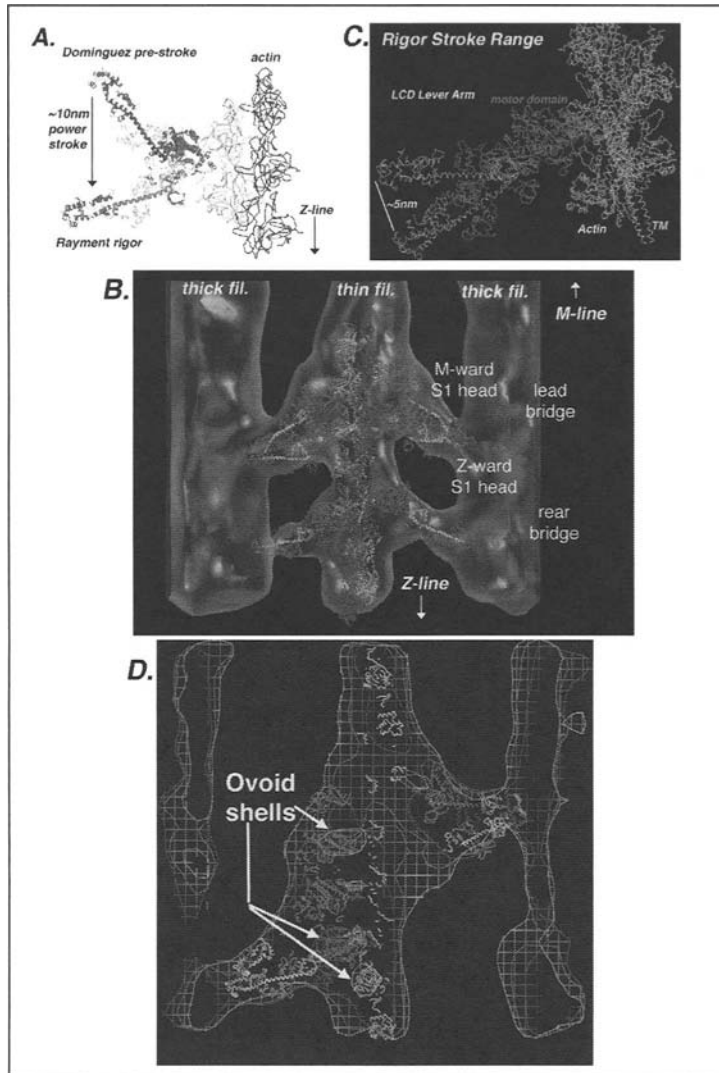


Figure 4. A) Superimposition of the crystal structures of the hypothesized prestroke and rigor S1 on the same motor domain docked on one actin protomer in the strong-binding rigor configuration. The atomic structure of chicken smooth myosin with ADP•AlF₄ bound,³⁶ was proposed to mimic the prepowerstroke shape of the head on actin (i.e., the “A•M•ADP•Pi” state, although in the absence of actin). With the actin filament axis vertical and the Z-band towards the bottom, the crystal structure of rigor S1 has the lever arm angled down at about 45°. A transition between these two forms would give a power stroke of ~10 nm. B) A class average from a tomogram of rigor IFM rendered in transparent envelope showing a double chevron and Rayment rigor S1s rebuilt to fit the crossbridge envelopes. Modified from Chen et al.⁴⁴ C) Superimposition of all S1s fitted to rigor crossbridges on one motor domain and actin shows a 5.8 nm range of LCD positions, implying a 5 nm lever arm swing during the transition into rigor. TM is tropomyosin. Actin strands are green/blue, the myosin motor domain is red, the LCD heavy chain is yellow, the converter domain is green, the ELC is purple, the RLC is brown. D) Slab through the central region of a white wireframe representation of a class average from a tomogram of stretched rigor IFM⁴⁵ showing the ovoid stain shells outlining the actin (green)/motor domain (red region). The thin slab includes different portions of the actin/motor domains at successive axial positions along the helical filament because successive actins are rotated ~25°. A color version of this figure is available online at <http://www.Eurekah.com>.

Correspondence class averages from tomograms of IFM rigor fibers fast frozen and freeze substituted after ramp stretches⁴⁵ showed actin filament substructure (Fig. 4D) for the first time in *averaged* images of IFM. This supports more precise alignment of the acto-S1 atomic models in the crossbridge envelopes (Fig. 5A-D). Original images and class averages also showed for the first time the position of a segment of S2 in some 38.7 nm crossbridge motifs (Fig. 5). Visualization of S2 allows us to estimate how close to bring the LCDs at the S1/S2 junction and how the “hook helices” must be directed in order to join the closely-spaced coiled-coil of S2. The atomic fittings of stretched rigor crossbridges (Fig. 5A,B) demonstrate that the LCD lever arm of the nucleotide-free S1 crystal structure³² lies outside the envelopes of rigor crossbridges. K843 at the end of the “hook” helix is much too far from K843 of the partner head to join the coiled-coil of S2 (Fig. 5A). The azimuthal position of Rayment S1³² diverges even more from *in situ* crossbridges, requiring very large azimuthal shifts of the lever arm to fit rear crossbridges (Fig. 5B compared to 5D). This large azimuthal distortion, which is typical of rear bridges, reflects their position at the edge of the actin target zone and can account for their variable occupancy and single-headedness in rigor.

The rationale for stretching rigor fibers was to explore the range of flexibility of strongly bound myosin heads: Could rigor crossbridges be “backbent” toward the M-line by a stretch, and if so, where, and by how much, do they bend? The average M-ward shift of rigor bridges in vertebrate muscle reported by X-ray diffraction was very small, compared to the larger amount of average M-ward movement detected in isometrically active muscle.^{46,47} Lui et al⁴⁵ found a variation in the amount of crossbridge response to stretch along the 116 nm long axial repeat of rigor IFM. In some class averages, crossbridge LCD lever arms were backbent M-ward by up to 4.5 nm (Fig. 4D), while the lever arm angles of other classes were the same as those from unstretched rigor class averages. In some class averages, apparent backbending in original EM images could be seen after atomic fitting to be largely due to the swing-out of a segment of S2 from the thick filament shaft. The exposure of S2 lends a very strong backbent appearance to the crossbridge in projection view, but does not actually involve extensive flexing of the lever arm toward the M-line (Fig. 5C). The *overall average* of M-ward shift of LCD lever arms from all class averages was only 1.4 nm, consistent with X-ray results from stretches of frog rigor muscle.⁴⁶⁻⁴⁸ But the overall average does not reveal the variation in crossbridge response to a change in load or the distribution of the variation along the thin filament.

Correspondence analysis not only improves the resolution of the averages, it allows the distribution and position of particular crossbridge conformations to be located in the large array of crossbridges in the sarcomere. “Mapbacks” replace each 38.7 nm crossbridge repeat in the tomogram by its class average (Fig. 5E). In stretched rigor, the variation in lever arm backbending was regularly distributed along the 116 nm long repeat (3 X 38.7 nm and 9 X 12.9 nm).^{45,49,50} In rigor, the variability in crossbridge form along the thin filament inherent to the varying register of myosin head origins and actin targets has been smoothed over by movements of the lever arms and S2 to yield a seamless 38.7 nm repeat of chevrons. Mapbacks of class averages reveal the hidden strain and distortion exposed by the stretch in rigor. This variation in crossbridge strain along the filament is important in active contraction.

Active Contraction

The ultimate goal has been to elucidate the 3D structure of myosin crossbridges as they generate force during an active contraction. But for many years, 3D visualization of actively contracting crossbridges has been limited by the variability of active myosin head conformations due to the mismatch between bridge origins and actin targets and the millisecond time resolution required to trap the stretch-activated contractions characteristic of IFM.

Isometric, Calcium Activated Contraction

In order to by-pass the stringent time constraints required to capture stretch activated contractions, isometric, calcium-activated contractions of glycerinated *Lethocerus* fibers were developed for structural studies as the high static tension or HST state.⁴¹ Stretch is unnecessary

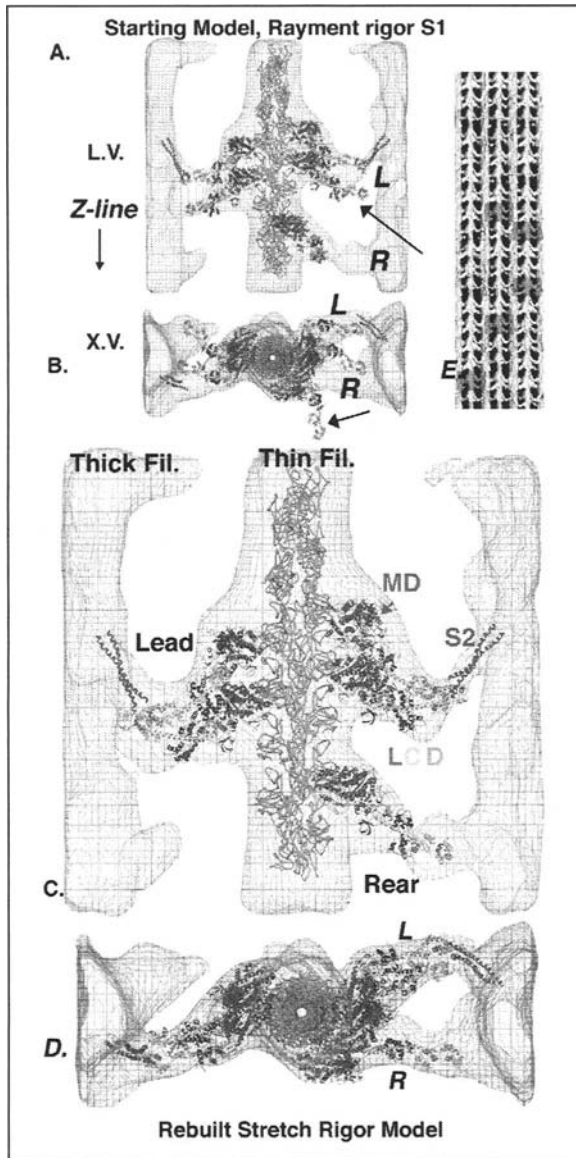


Figure 5. A-D) One class average from a tomogram of fast frozen, stretched rigor IFM comparing the unmodified (A,B) and rebuilt (C,D) atomic models of rigor S1³² and the relation of the S1s to S2 (~50 residue segment, 7 heptads, magenta). A) Longitudinal view (L.V.) of unmodified rigor S1. The LCD lever arm often lies outside the bridge envelope (arrow) and clearly, the LCDs are too far apart to form a vertex at the junction with S2. Actin filament is green. B) Cross section view (X.V.) of Lead bridges (L) shown in panel (A). The unmodified S1 crystal structure lies far outside the bridge envelope particularly at the rear bridge (R). C) The crystal structure of Rayment S1 was rebuilt to fit the bridge envelope by pivoting about three residues, G710 between the motor (MD) and converter (green) domains, D780 between the converter and ELC (blue) and M806 between the ELC and RLC (cyan). D) Cross section view of (C). E) Small area from a "mapback" of a stretch rigor tomogram in surface rendering showing some examples (red squares) of the distribution of the class average shown in panels (A-D). Data from Liu et al.⁴⁵ A color version of this figure is available online at <http://www.Eurekah.com>.

for HST; in the presence of $\text{Mg}\cdot\text{ATP}$, raising $[\text{Ca}^{2+}]$ to >0.1 mM (pCa 4.5) produces strong isometric contraction that can last for many seconds. In vivo, prolonged isometric contraction by flight muscles is used for thermogenesis in the preflight warmup that brings IFM to -40°C , as required for flight in most larger insects.⁵¹

Figure 6 illustrates a general overview of tomography and atomic model fitting of IFM of the isometric HST state.⁴¹ EM tomograms of isometrically-activated IFM freeze-substituted after rapid freezing show well-ordered, single headed cross-bridges binding in actin target zones with a wide range of attachment angles, from prestroke to rigor-like end-stroke.⁴¹ The variation in bridge angle appeared to correlate with the varying alignment of the actin target zones every 38.7 nm with the crossbridge origins every 14.5 nm. Actin targets and bridge origins go through a match/mismatch alignment every 116 nm (3×38.7 nm and 8×14.5 nm) along the thin filament in active IFM. Therefore, the signal to noise in the raw unaveraged tomogram was improved without averaging across the variable crossbridge array over the sarcomere, by averaging along each thick-thin column (column averaging) to reduce each thin filament to a single average 116 nm long repeat. The column averages showed that there was always at least one pair of crossbridges bound in a narrow actin target zone midway between the head regions of the troponin complex every 38.7 nm and one more crossbridge attached in the target zone in one or two of the three 38.7 nm repeats. The angles of isometric crossbridges varied from $>100^\circ$ (antirigor) in bridges that originated on the M-ward side of the target zone center, to rigor-like ($\sim 45^\circ$) in bridges originating on the Z-ward side of target zone center in each 38.7 nm repeat.

Rebuilding acto-S1 models to fit isometrically active crossbridge envelopes required various axial and azimuthal adjustments of the Rayment starting S1 crystal model⁴¹ (Fig. 6). The active bridges near the rigor angle ("end stroke") needed only small azimuthal adjustments of the lever arm angle of the S1 model, while bridges at intermediate axial angles between $\sim 60^\circ$ to $\sim 100^\circ$ required larger adjustments of the LCD lever arm position. The "antirigor" angle ($>100^\circ$) crossbridges could not be fitted with a lever arm adjustment of rigor S1. These putative "prestroke" bridges also required shifting the motor domain of rigor S1 M-ward of its position and very large M-ward tilting of the S1 lever arm to fit the envelope of the crossbridge. A crystal structure of S1 with bound nucleotide proposed to be in the "prestroke" conformation⁵² was a closer match to the "antirigor" crossbridges. However, the motor domain of "prestroke" S1 was oriented on actin in the rigor position and did not precisely match the nonrigor position of the "anti-rigor" crossbridges.

The rebuilt acto-S1 atomic models suggested a two stage power stroke, in which the motor domain tilts on actin from a "weak" binding position to the strong rigor position, followed by tilting of the LCD lever arm from a prepower stroke position at high angle to a rigor position near 45° . Several models propose that following attachment to actin, tilting of the LCD can produce a ~ 10 -11 nm working stroke, while the motor domain maintains a relatively constant rigor-like orientation.^{37,38,53} The crossbridges in which the motor domain is not at the rigor position on actin and the lever arm is up at a high angle may represent weak contacts between myosin and actin at the beginning of a power stroke that realign on actin to reach a strong binding position. Or, they may be nonstereospecific contacts that do not evolve into force producing interactions.

The range of rebuilt S1 models in HST was ordered into a hypothetical sequence compatible with a continuously attached, progressive ~ 12 nm power stroke comprising an angular range of $>100^\circ$ to 45° .⁴¹ However, the frequency and distribution of cross-bridge positions and angles within the full range were not determined.

Analysis of the tomograms of isometrically active IFM was extended to quantify the distribution and orientation of attached cross-bridges during isometric contractions.⁵⁴ The number and position of attached myosin heads were measured by tracing cross-bridges through the 3-D tomogram from their origins on 14.5 nm spaced shelves along the thick filament to their attachments in the actin target zones every 38.7 nm. Surprisingly, the frequency of crossbridge binding to actin plotted relative to the axial distance between the center of the actin target zone

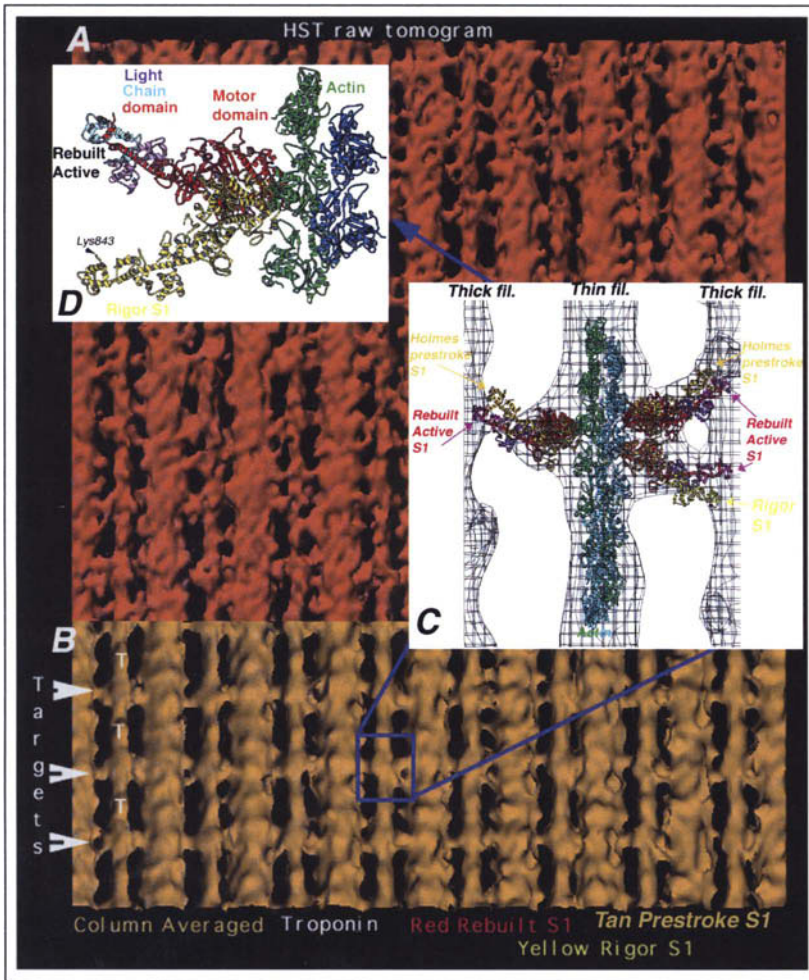


Figure 6. Summary of tomography and atomic model building of the calcium-activated, isometric high static tension (HST) state of *Lethocerus* IFM from Taylor et al.⁴¹ A) Unaveraged (raw) tomogram (orange) of HST in surface rendering is very noisy. B) "Column averaging" (yellow) of each thin filament and crossbridges reduces each filament to three 38.7 nm averaged motifs (an 116 nm repeat) that reduces noise while retaining natural crossbridge variability. "Targets" indicate the actin target zones midway between troponins (T). The blue rectangle outlines the motif enlarged in (C). C) Wireframe rendering of an averaged 38.7 nm crossbridge motif (blue box) from the tomogram of the isometric HST state showing fitted active S1 in red. Unaltered Rayment rigor S1³² in yellow is superimposed on the Z-ward bridge and unaltered Holmes prestroke S1 (tan)⁵² is superimposed on the more M-ward bridges. D) One of the "prestroke" fitted S1 (red) and one of the fitted rigor-angled HST S1 are shown bound to the same actin to illustrate the range of observed myosin head angles in isometric contraction.

and the bridge origin showed a Gaussian distribution. The majority of isometric crossbridges are nearly perpendicular to the filaments (60% within 11°) with lower and equal numbers of bridges at prestroke and rigor angles. The results suggest that when the filaments cannot slide, individual cross-bridges generate tension with little change in axial translocation or angle.

Fast force transients and X-ray diffraction of vertebrate fibers also indicate the average bridge angle in isometric contraction is close to 90°. In isometrically active frog muscle, the behaviour of the 14.5 nm meridional X-ray reflection is best modelled with cross-bridges nearly perpendicular to the filaments.^{47,46} X-ray interferometry indicates that in skeletal muscle at high load, the length of the myosin power stroke is short⁵⁵ and most tension-generating bridges are close to perpendicular to the filament axis.

Force generation with little or no lever-arm tilt suggests a flexing cantilever action of the lever arm, similar to the bending of a fishing pole when the hook is lodged in a very heavy load.^{56,47} Such flexing is seen in class averages of stretched rigor (Fig. 5).

Stretch Activation

An important long-standing question about IFM has been whether stretch activation involves a fundamentally different mechanism than calcium activation. Recent studies of *Lethocerus* IFM have examined the relationship between Ca⁺⁺-activated isometric contraction and stretch activation.

Physiological experiments indicate that Ca⁺⁺-activation and stretch-activation are complementary mechanisms that trigger a common process of crossbridge attachment and force production.⁵⁷ In the absence of any stretch, at high calcium concentration (pCa4.5) *Lethocerus* IFM can reach nearly its maximum force (80 kN m⁻²). A minimum amount of tension (5-10% of maximum) and crossbridge attachment must be activated by Ca⁺⁺ in order to obtain stretch activation. The amount of increased force obtained after stretch is greatest when calcium-activated isometric force is ~20% of maximum. The amount of stretch-activated tension decreases as the starting Ca⁺⁺-activating tension increases to produce a nearly constant sum of isometric Ca⁺⁺ activated and stretch-activated tension. Linari et al⁵⁷ propose that stretch distorts the requisite small number of crossbridges attached in response to a low level of calcium activation. The stretch induced distortion of initially attached crossbridges displaces tropomyosin (Tm) over a longer stretch of actin and opens many more sites for more crossbridge attachment, without requiring Ca⁺⁺/troponin induced movement of tropomyosin along the full length of the thin filament.

Other recent experiments have characterized two different isoforms of TnC in *Lethocerus* that suggest that the Tn/Tm regulatory system is adapted to allow stretch to trigger full crossbridge attachment and high force at [Ca⁺⁺] that are too low to fully activate the muscle.^{58,59} Agianian et al⁵⁹ propose that the special troponin is somehow mechanically activated by stretch. EM images of ATP-relaxed *Lethocerus* IFM, like those in Figure 1, show that the most prominent bridging bars in relaxed IFM are aligned with the troponin densities every 38.7 nm. This suggests the possibility that these relaxed myosin/actin/troponin contacts are activated at low calcium concentration and distortion of these myosin heads by stretch mechanically activates the troponin/tropomyosin system along the entire thin filament, allowing rapid crossbridge attachment in actin target zones all along the thin filaments.

Our first glimpses of stretch activated crossbridge structure and arrangement have been enabled by advances in time-resolved fast freezing and synchrotron X-ray diffraction. Time-resolved X-ray diffraction of IFM during stretch activated contractions⁶⁰ provided evidence that myosin crossbridges attach preferentially to actin target zones midway between troponin head regions every 38.7 nm. Stretch-activation triggered by step stretches of *Lethocerus* IFM poised at the lowest threshold of calcium-activated force gave a large rise in active tension that peaked in 100-200 ms. The intensities of the lattice-sampled peaks of the pattern changed as active tension rose: the 14.5 and 7.2 nm meridionals fell, a first row line peak became visible on the 19.3 nm layer line, and the first row line peak on the 38.7 nm layer line fell. Tregear et al⁶⁰ concluded that stretch-activated tension under these conditions is produced by the binding of between 16-25% of the total number of myosin heads in IFM.

Electron micrographs of 25 nm longitudinal sections of stretch-activated IFM fibers at low calcium concentration, fast frozen at the plateau of tension (200 ms), and freeze substituted

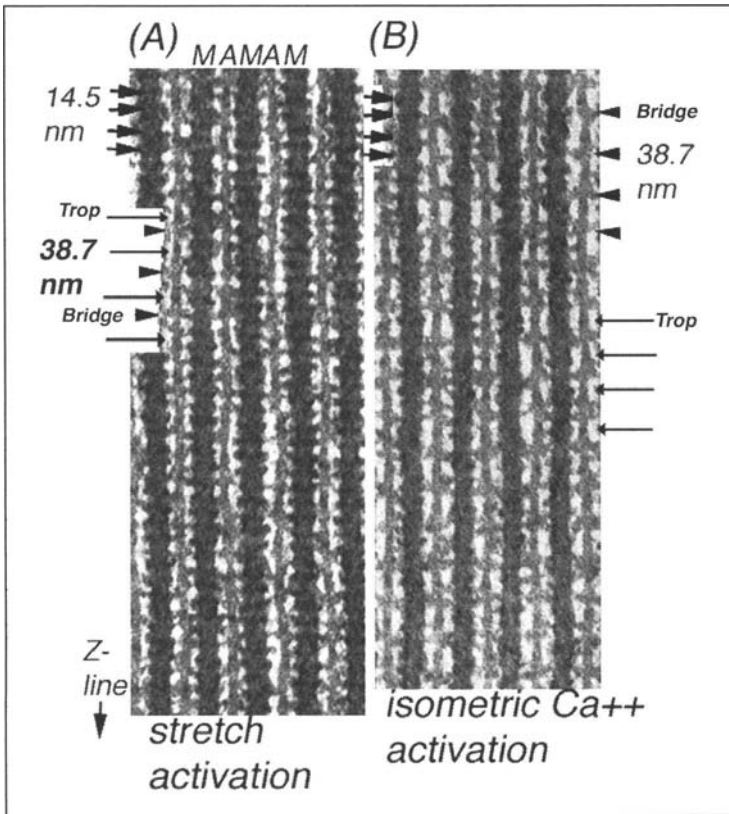


Figure 7. Electron micrographs of myac layers of stretch activated (A) and isometric HST (B) *Lethocerus* IFM. Note the prominence of the 14.5 nm shelves (short arrows) on the thick filaments at the plateau of stretch-activated tension compared to those in HST (short arrows in B). The regularity and number of crossbridges binding to actin is greater in HST, consistent with more heads moving out from the 14.5 nm shelves in HST. However, in both HST and stretch activation, bridges bind primarily in actin target zones every 38.7 nm (arrowheads), midway between troponin densities (trop, long arrows) also distributed every 38.7 nm. In (A), the arrows highlighting this alternating pattern of crossbridge (bridge) binding (arrowheads) with troponin density (long arrows, trop) are shown in sequence, while in (B) bridge and troponin arrows are shown separately. M is myosin filament; A is actin filament.

and epoxy embedded (Fig. 7A), show single myosin heads at varying angles attaching preferentially in actin target zones every 38.7 nm along thin filaments, in agreement with X-ray diffraction patterns. In contrast to rigor crossbridges, stretch activated bridges were single headed and very few were at or near the classical “45°” rigor bridge angle. Compared to isometrically active IFM (Fig. 7B), fewer crossbridges are bound to actin in stretch activation and the 14.5 nm shelves along the thick filament remain very prominent, indicating that many myosin heads are not attached to actin. However, stretch activated IFM exemplifies the difficulties in analyzing 3D structural details in crossbridge states that display a large variation in crossbridge forms and have a large population of myosin heads that are not attached to actin and remain related to the thick filament. Until very recently, there were no models for the disposition of myosin heads along the *Lethocerus* thick filament.

The ATP-Relaxed State

The conformation and arrangement of myosin heads in ATP relaxed muscle is important as the departure point for active contraction. In ATP-relaxed *Lethocerus* IFM, the shelves of density every 14.5 nm project from the thick filament toward actin at a 90° axial angle. The “right angle” appearance of the 14.5 nm crown shelves in electron micrographs and tomograms naturally suggested that relaxed myosin heads project toward actin at a 90° axial angle. However, X-ray modeling has recently revealed a surprising arrangement of the myosin heads in each 14.5 nm shelf.⁶¹

X-ray diffraction patterns from relaxed IFM have been modelled by testing which shape and arrangement of the 8 heads in a 14.5 nm shelf gave diffraction that best matched the native X-ray pattern. The different head shapes were obtained by pivoting the myosin head atomic coordinates around a hinge between the motor domain and the LCD lever arm. The myosin head shape that best matched the relaxed X-ray pattern (Fig. 8) resembled the crystal structure of S1 thought to be in a “prepower stroke” conformation.³⁴ In this configuration, the lever arm of the S1 is angled “up” relative to the motor domain, instead of angling “down” toward the Z-band, as in rigor, or projecting straight off the motor domain, as in Houdusse et al.³⁵ In the X-ray model, both heads of one myosin molecule assume the identical prestroke shape, but they adopt nonequivalent positions. One head projects out from the thick filament surface, emphasizing the projecting shelves of density seen in electron micrographs, while the second “inner” head curves circumferentially around the backbone to bring its ATP-binding cleft into contact with the LCD of the projecting head of an adjacent myosin molecule (Fig. 8). This differs from the contact between coheads within unphosphorylated smooth muscle heavy meromyosin (smHMM),⁶² where the actin binding region of one head contacts the converter domain of the cohead. In IFM, the inner head tucked in behind the projecting head could act to maintain the position of the projecting head and stabilize the relaxed head arrangement. The LCD/ATP site contact in relaxed IFM could inhibit the ATPase of the inner head in the resting state and possibly also the activity of the projecting head.

The prestroke conformation of the myosin heads in ATP-relaxed *Lethocerus* IFM is consistent with data that the myosin head is cocked in an “up” conformation while detached from actin.⁶³ The nonrigor orientation of the actin binding cleft in the relaxed X-ray model (Fig. 8) suggests that a twisting movement of the motor domain or whole head may be needed to align the cleft for strong binding to actin. This realignment may be related to the twist of the lever arm observed during contraction in bi-functional probe experiments.^{64,65} It is also consistent with the nonrigor orientation of the motor domain in highly angled “prestroke” bridges in isometrically contracting IFM.⁴¹

Concluding Remarks

The newer picture of the myosin power stroke suggests that the internal structure of the myosin head can drive large angle changes and 5-12 nm strokes, but, in situ, the length of the power stroke depends on the load. At high load, myosin molecules can generate force with very little change of angle, probably by a flexing of the lever arm. Rapid length and tension transients superimposed on isometrically active IFM are needed to explore the range of myosin lever arm positions associated with changes in load or length. Applying elastic network and normal mode analysis⁶⁶ to model building holds promise for defining the elastic deformation of crossbridges. Further improvement in correspondence analysis averaging is essential for atomic model building of crossbridges in tomograms of stretch-activated contractions. Mapbacks of correspondence class averages hold promise for defining the distribution of crossbridge conformations and strain in sarcomeres and should contribute insight into strain-dependent processes, such as ADP release,^{67,68} that are increasingly recognized as central to myosin motor function.

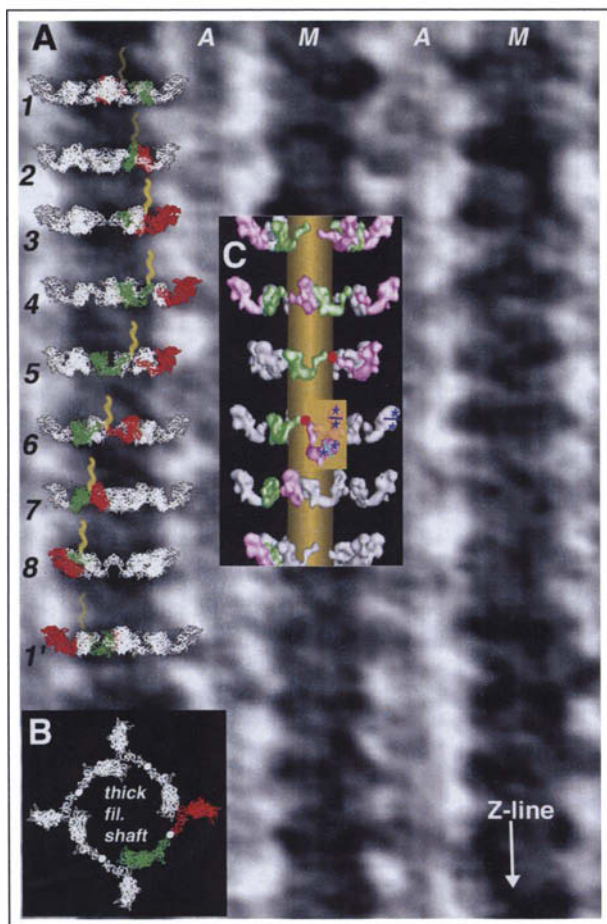


Figure 8. The myosin head conformation and arrangement that best matches the X-ray pattern of ATP-relaxed *Lethocerus* IFM. A) Thick filaments in a highly enlarged electron micrograph of a myac layer section of relaxed IFM are overlaid at approximately the same scale by crowns of S1 (numbered 1-8) whose prestroke conformation and arrangement fits the X-ray pattern.⁶¹ Each crown is rotated 33.75° at successive 14.5 nm shelf levels. Eight 14.5 nm levels are equal to 116nm; the ninth level (1') rotation is superimposable on crown level (1). The yellow squiggly line indicates the direction of S2 along the thick filament shaft and is only illustrated for the single myosin molecule whose heads are shown in red and green, to emphasize the helical tracks formed by the red and green heads. All S1 are in the same "prestroke" conformation, but the projecting head (red) shows this more clearly than in inner head (green). B) "Cross section" view of one crown/shelf at the same rotation as level 4 in (A). The heads of one molecule are colored, the heads of the other three molecules at each level are white. The S2 joining coheads of one molecule are solid white circles. C) A surface rendering of the myosin heads in the best fit arrangement showing six 14.5 nm shelf levels, each rotated 33.75° , is shown over a gold thick filament shaft. In one myosin molecule at each level, the projecting head is pink and the inner head is green. The other three heads are white. At the same level as shelf six on the adjacent filament in (A), blue stars flank bars that indicate the orientation of the actin binding cleft of myosin. In the yellow box, the position of the cleft that matches the strong-binding rigor position is indicated by the cyan bar on the pink head. This projecting head, still in the prestroke conformation, has been shifted from its relaxed position (pale yellow, horizontal bar/cleft) by rotating around its junction with S2 (red dot) to orient its actin binding cleft in the strongly bound position on actin without changing the "prestroke" conformation of the head. The actin binding cleft of the projecting white head would need to be rotated $\sim 60^\circ$ by a twist of some part, or all, of the myosin head in order to orient in the strong binding position on actin.

Acknowledgements

The preparation of this paper was supported by NIH grant R01AR14317 to M.K. Reedy.

References

1. Irving TC, Maughan DW. In vivo X-ray diffraction of indirect flight muscle from *Drosophila melanogaster*. *Biophys J* 2000; 78(5):2511-2515.
2. Reedy MC, Beall C. Ultrastructure of developing flight muscle in *Drosophila*. I. Assembly of myofibrils. *Dev Biol* 1993; 160:443-465.
3. Reedy MC, Beall C. Ultrastructure of developing flight muscle in *Drosophila*. II. Formation of the myotendon junction. *Dev Biol* 1993; 160:466-479.
4. Emerson Jr CP, Bernstein SI. Molecular genetics of myosin. *Annu Rev Biochem* 1987; 56:695-726.
5. Bernstein SI, Milligan RA. Fine tuning a molecular motor: The location of alternative domains in the *Drosophila* myosin head. *J Mol Biol* 1997; 271:1-6.
6. Becker KD, Bernstein SI. Genetic and transgenic approaches to dissecting muscle development and contractility using the *Drosophila* model system. *Trends Cardiovasc Med* 1994; 4:243-250.
7. Fyrberg EA. Genetic and molecular analyses of *Drosophila* contractile protein genes. *BioEssays* 1986; 2:250-254.
8. Fyrberg EA, Mahaffey JW, Bond BJ et al. Transcripts of the six *Drosophila* actin genes accumulate in a stage- and tissue-specific manner. *Cell* 1983; 33:115-123.
9. Nongthomba U, Cummins M, Clark S et al. Suppression of muscle hypercontraction by mutations in the myosin heavy chain gene of *Drosophila melanogaster*. *Genetics* 2003; 164(1):209-222.
10. Reedy MC, Beall C, Fyrberg EA. Formation of reverse rigor chevrons by myosin heads. *Nature* 1989; 339:481-483.
11. Dickinson MH, Hyatt CJ, Lehmann FO et al. Phosphorylation-dependent power output of transgenic flies: An integrated study. *Biophys J* 1997; 73(6):3122-3134.
12. Sparrow J, Reedy MC, Ball E et al. Functional and ultrastructural effects of a missense mutation in the indirect flight muscle-specific actin gene of *Drosophila melanogaster*. *J Mol Biol* 1991; 222:963-982.
13. Fyrberg E, Kelly M, Ball E et al. Molecular genetics of *Drosophila* alpha-actinin: Mutant alleles disrupt Z disc integrity and muscle insertions. *J Cell Biol* 1990; 110:1999-2011.
14. Brault V, Sauder U, Reedy MC et al. Differential epitope tagging of actin in transformed *Drosophila* produces distinct effects on myofibril assembly and function in indirect flight muscles. *Mol Biol Cell* 1999; 10(1):135-149.
15. Cripps RM, Becker KD, Mardahl M et al. Transformation of *Drosophila melanogaster* with the wild-type myosin heavy-chain gene: Rescue of mutant phenotypes and analysis of defects caused by overexpression. *J Cell Biol* 1994; 126:689-699.
16. Reedy MC, Bullard B, Vigoreaux JO. Flightin is essential for thick filament assembly and sarcomere stability in *Drosophila* flight muscles. *J Cell Biol* 2000; 151(7):1483-1500.
17. Reedy MK, Holmes KC, Tregear RT. Induced changes in orientation of the cross-bridges of glycinated insect flight muscle. *Nature* 1965; 207:1276-1280.
18. Huxley HE. The mechanism of muscular contraction. *Sci Am* 1965; 213:18-27.
19. Huxley HE, Hanson J. Changes in the cross-striations of muscle during contraction and stretch and their structural interpretation. *Nature* 1954; 173:973-976.
20. Huxley AF, Niedergerke R. Structural changes in muscle during contraction. *Nature* 1954; 173:971-973.
21. Huxley AF, Simmons RM. Proposed mechanism of force generation in striated muscle. *Nature* 1971; 233:533-538.
22. Huxley HE. The structural basis of muscular contraction. *Proc R Soc Lond B: Biological* 1971; 178:131-149.
23. Reedy MK, Squire JM, Baumann BAJ et al. X-ray fiber diffraction of the indirect flight muscle of *Lethocerus indicus*. *Advanced Photon Source User Activity: Report 2000*. Argonne: Argonne National Laboratory, 2000.
24. Schmitz H, Reedy MC, Reedy MK et al. Electron tomography of insect flight muscle in rigor and AMPPNP at 23°C. *J Mol Biol* 1996; 264:279-301.
25. Schmitz H, Reedy MC, Reedy MK et al. Tomographic three-dimensional reconstruction of insect flight muscle partially relaxed by AMPPNP and ethylene glycol. *J Cell Biol* 1997; 139:695-707.
26. Reedy MC. Visualizing myosin's power stroke in muscle contraction. *J Cell Sci* 2000; 113:3551-3562.
27. Taylor KA, Tang J, Cheng Y et al. The use of electron tomography for structural analysis of disordered protein arrays. *J Struct Biol* 1997; 120:372-386.

28. Frank J, ed. *Electron Tomography: Three-dimensional imaging with the transmission electron microscope*. New York: Plenum Press, 1992.
29. Schmitz H, Reedy MC, Reedy MK et al. Tomographic 3D-reconstruction of insect flight muscle in rigor and aqueous AMPPNP. *J Muscle Res Cell Motil* 1996; 17(1):119-119.
30. Winkler H, Taylor KA. Multivariate statistical analysis of three-dimensional cross-bridge motifs in insect flight muscle. *Ultramicroscopy* 1999; 77(3-4):141-152.
31. Himmel DM, Gourinath S, Reshetnikova L et al. Crystallographic findings on the internally uncoupled and near-rigor states of myosin: Further insights into the mechanics of the motor. *Proc Natl Acad Sci USA* 2002; 99(20):12645-12650.
32. Rayment I, Rypniewsky WR, Schmidt-Bäse K et al. Three-dimensional structure of myosin subfragment-1: A molecular motor. *Science* 1993; 261:50-58.
33. Fisher AJ, Smith CA, Thoden JB et al. X-ray structures of the myosin motor domain of *Dictyostelium discoideum* complexed with $MgADP \cdot BeF_x$ and $MgADP \cdot AlF_4^-$. *Biochemistry* 1995; 34:8960-8972.
34. Dominguez R, Freyzon Y, Trybus KM et al. Crystal structure of a vertebrate smooth muscle myosin motor domain and its complex with the essential light chain: Visualization of the pre power stroke state. *Cell* 1998; 94:559-571.
35. Houdusse A, Kalabokis VN, Himmel D et al. Atomic structure of scallop myosin subfragment S1 complexed with $MgADP$: A novel conformation of the myosin head. *Cell* 1999; 97:459-470.
36. Gulick AM, Bauer CB, Thoden JB et al. X-ray structures of the *Dictyostelium discoideum* myosin motor domain with six nonnucleotide analogs. *J Biol Chem* 2000; 275(1):398-408.
37. Rayment I, Holden HM, Whittaker M et al. Structure of the actin-myosin complex and its implications for muscle contraction. *Science* 1993; 261:58-65.
38. Holmes KC. The swinging lever-arm hypothesis of muscle contraction. *Curr Biol* 1997; 7:R112-118.
39. Jontes JD, Wilson-Kubalek EM, Milligan RA. A 32° tail swing in brush border myosin I on ADP release. *Nature* 1995; 378:751-753.
40. Whittaker M, Wilson-Kubalek EM, Smith JE et al. A 35-Å movement of smooth muscle myosin on ADP release. *Nature* 1995; 378:748-751.
41. Taylor KA, Schmitz H, Reedy MC et al. Tomographic 3-D reconstruction of quick frozen, Ca^{2+} -activated contracting insect flight muscle. *Cell* 1999; 99:421-431.
42. Reedy MK, Reedy MC. Rigor crossbridge structure in tilted single filament layers and flared-X formations from insect flight muscle. *J Mol Biol* 1985; 185:145-176.
43. Frank J, van Heel M. Correspondence analysis of aligned images of biological particles. *J Mol Biol* 1982; 161:134-137.
44. Chen LF, Winkler H, Reedy MK et al. Molecular modeling of averaged rigor crossbridges from tomograms of insect flight muscle. *J Struct Biol* 2002; 138:92-104.
45. Liu J, Reedy MC, Goldman YE et al. Electron tomography of fast frozen, stretched rigor fibers reveals elastic distortions in the myosin crossbridges. *J Struct Biol* 2004; 147(3):268-282.
46. Irving M, Piazzesi G, Lucii L et al. Conformation of the myosin motor during force generation in skeletal muscle. *Nat Struct Biol* 2000; 7(6):482-485.
47. Dobbie I, Linari M, Piazzesi G et al. Elastic bending and active tilting of myosin heads during muscle contraction [see comments]. *Nature* 1998; 396:383-387.
48. Reconditi M, Dobbie I, Irving M et al. Myosin head movements during isometric contraction studied by X-ray diffraction of single frog muscle fibres. *Adv Exp Med Biol* 1998; 453:265-270.
49. Crowther RA, Luther PK, Taylor KA. Computation of a three dimensional image of a periodic specimen from a single view of an oblique section. *Electron Microsc Rev* 1990; 3:29-42.
50. Schmitz H, Lucaveche C, Reedy MK et al. Oblique section 3-D reconstruction of relaxed insect flight muscle reveals the cross-bridge lattice in helical registration. *Biophys J* 1994; 67:1620-1633.
51. Heinrich B. *The thermal warriors. Strategies of insect survival*. Cambridge: Harvard University Press, 1996.
52. Holmes KC. Muscle proteins—their actions and interactions. *Curr Opin Struct Biol* 1996; 6:781-789.
53. Holmes KC. A molecular model for muscle contraction. *Acta Crystallogr A* 1998; 54:789-797.
54. Tregear RT, Reedy MC, Goldman YE et al. Cross-bridge number, position and angle in target zones of cryofixed isometrically active insect flight muscle. *Biophys J* 2004; 86(5):3009-3019.
55. Reconditi M, Linari M, Lucii L et al. The myosin motor in muscle generates a smaller and slower working stroke at higher load. *Nature* 2004; 428(6982):578-581.
56. Goldman YE. Wag the tail: Structural dynamics of actomyosin. *Cell* 1998; 93:1-4.
57. Linari M, Reedy MK, Reedy MC et al. Ca-activation and stretch-activation in insect flight muscle. *Biophys J* 2004; 87(2):1101-1111.

58. Qiu F, Lakey A, Agianian B et al. Troponin C in different insect muscle types: Identification of two isoforms in *Lethocerus*, *Drosophila* and *Anopheles* that are specific to asynchronous flight muscle in the adult insect. *Biochem J* 2003; 371(Pt 3):811-821.
59. Agianian B, Krzic U, Qiu F et al. A troponin switch that regulates muscle contraction by stretch instead of calcium. *EMBO J* 2004; 23:772-779.
60. Tregear RT, Edwards RJ, Irving TC et al. X-ray diffraction indicates that active crossbridges bind to actin target zones in insect flight muscle. *Biophys J* 1998; 74:1439-1451.
61. AL-Khayat HA, Hudson L, Reedy MK et al. Myosin head configuration in relaxed insect flight muscle: X-ray modelled resting crossbridges in a prepowerstroke state are poised for actin binding. *Biophys J* 2003; 85(2):1063-1079.
62. Wendt T, Taylor D, Trybus KM et al. Three-dimensional image reconstruction of dephosphorylated smooth muscle heavy meromyosin reveals asymmetry in the interaction between myosin heads and placement of subfragment 2. *Proc Natl Acad Sci USA* 2001; 98(8):4361-4366.
63. Geeves MA, Holmes KC. Structural mechanism of muscle contraction. *Annu Rev Biochem* 1999; 68:687-728.
64. Corrie JE, Brandmeier BD, Ferguson RE et al. Dynamic measurement of myosin light chain domain tilt and twist in muscle contraction. *Nature* 1999; 400(6743):425-430.
65. Hopkins SC, Sabido-David C, van der Heide UA et al. Orientation changes of the myosin light chain domain during filament sliding in active and rigor muscle. *J Mol Biol* 2002; 318(5):1275-1291.
66. Tama F, Brooks C. Normal mode based flexible fitting of high-resolution structure into low-resolution experimental data from cryo-EM. *J Structural Biology* 2004; in press.
67. Smith DA, Geeves MA. Strain-dependent cross-bridge cycle for muscle. *Biophys J* 1995; 69:524-537.
68. Cremo CR, Geeves MA. Interaction of actin and ADP with the head domain of smooth muscle myosin: Implications for strain-dependent ADP release in smooth muscle. *Biochemistry* 1998; 37:1969-1978.
69. Irving TC, Fischetti R, Rosenbaum G et al. Fiber diffraction using the BioCAT undulator beamline at the advanced photon source. *Nuclear Instruments and Methods (A)*. 2000; 448:250-254.

Nature's Versatile Engine:
Insect Flight Muscle Inside and Out
Vigoreaux, J. (Ed.)
2006, XXII, 288 p., Hardcover
ISBN: 978-0-387-25798-3